# A new mixed-ligand Mn(II) coordination polymer: Protective and nursing values on renal calculus via reducing the $Ca^{2+}$ concentration in urine

Yan Yang[1], Sheng-Mei Zhang[2], Yi-Qian Zhang[2], Liang Chen[3] and Tao Xiong[3]

## Abstract

In the present study, via using the mixed-ligand synthesis approach, a new Mn(II)-containing co-ordination polymer (CP) with the chemical formula of $\{[Mn_3(timb)_2(SO_3–IPA)_2(H_2O)_2]\cdot 8H_2O\}_n$ (1) has been successfully prepared via reaction of $MnCl_2\cdot 4H_2O$ with the tripodal linker 1,3,5-tris(2-methylimidazole-1-yl)benzene (timb) and aromatic dicarboxylic acid ligand $–SO_3$ group functionalized isophthalic acid ($H_2IPA$) ligand. Furthermore, the biological activity of the new compound on renal calculus was assessed, and the related mechanism was explored as well. The Calcium Colorimetric Assay was conducted and the concentration of $Ca^{2+}$ in urine was determined. The western blotting assay was conducted and the expression levels of the osteopontin (OPN) in the distal tubule were measured. Molecular docking simulation revealed that the carboxyl, iminazole, and sulfonate groups were all involving into the binding interactions with the target protein, and therefore exhibited strong biological activity.

## Keywords

Coordination complex, renal calculus, urine, molecular docking

[1]Hospital Office, Hanzhong Central Hospital, Hanzhong, China
[2]The Fourth Department of Health Care, Qingdao Municipal Hospital, Qingdao, China
[3]Department of Medicine, People's Hospital, Chongqing, China

**Corresponding author:**
Yi-Qian Zhang, The Fourth Department of Health Care, Qingdao Municipal Hospital, Qingdao 199232, China.
Email: zhangyiqian_1983@163.com

## Introduction

Recently, transition metal complexes containing inorganic metal ions and organic ligands have become the focus of interest due to not only their structural versatility but also their wide range of applications such as antitumor and antibacterial activities, insulin mimetic activities, luminescence properties, catalytic activities, magnetic properties, DNA binding properties, and gas adsorption.[1–6] It is well known that the structural versatility and activity properties of the metal–organic complexes are largely dependent on the choice of organic ligands and metal atoms used, as well as the reaction mechanism in which the complex is obtained.[7–10] Consequently, the logical design of the organic ligands and the selection of suitable metal ions play a key role in obtaining the coordination complexes with the desired properties. Manganese is the second most abundant transition metal within the Earth's crust. It is used to form oxygen in photosynthesis, an indispensable process for plant growth, and is involved in the absorption of nitrates in green plants and algae. In organisms having transactions with elemental oxygen, manganese enzymes are very imperative for the de-toxification of superoxide free radicals.[11–14] This metal carries out a variety of redox functions in living systems, like reduction of ribonucleotides to deoxyribonucleotides in coryneform bacteria and the disproportionation of hydrogen peroxide (catalase activity) in microorganisms. In biological system of higher animals, manganese(II) ions play a key role in the action of many enzymes and as a result there are a number of metalloproteins which necessitate manganese to execute their biological functions, and these have become important targets for synthetic modeling studies. Based on the above considerations, in the present study, via using the mixed-ligand synthesis approach, a new Mn(II)-containing coordination polymer (CP) with the chemical formula of $\{[Mn_3(timb)_2(SO_3–IPA)_2(H_2O)_2]\cdot 8H_2O\}_n$ (1) has been successfully prepared via reaction of $MnCl_2\cdot 4H_2O$ with the tripodal linker 1,3,5-tris(2-methylimidazol-1-yl)benzene (timb) and aromatic dicarboxylic acid ligand $–SO_3$ group functionalized isophthalic acid ($H_2IPA$, Scheme 1) ligand. The as-prepared coordination polymer 1 has been structurally studied via the single crystal X-ray diffraction and was further characterized by elemental analysis. Its treatment activity on the renal calculus was evaluated and the detail mechanism of the novel compound was discussed at the same time. Polar groups like carboxyl and iminazole groups are active to the polar hydrogens and cloud form hydrogen bonding interactions; thus, these two types of groups are common in the design of drug molecule against the related diseases. In the current study, the newly synthesized Mn complex contains multiple carboxyl and iminazole groups, besides, it also contains a sulfonate group, so the molecule is expected to form multiple interactions with the protein and represent good biological activity. In order to understand the underlying interacting mechanism, molecular docking simulation has been performed.
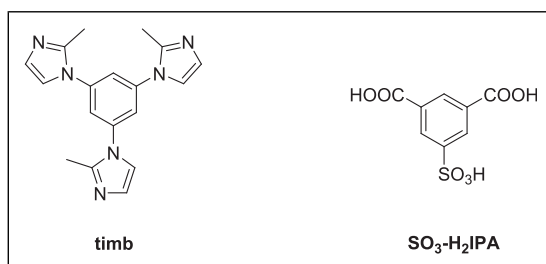


**Scheme 1.** The chemical drawings for the ligands.

## Experimental

### Chemicals and measurements

The two ligands used in this work were purchased from Jinan Henghua Sci. & Tec. Co. Ltd. Other materials were commercially available and used without further purification. Elemental analyses for C, H, and N were carried out on a Vario MACRO cube elemental analytical instrument. IR spectra were performed on an FTIR–8400S Spectrometer within the 4000–400 cm$^{-1}$ range in KBr pellets.

### Preparation and characterization for $\{[Mn_3(timb)_2(SO_3–IPA)_2(H_2O)_2]\cdot 8H_2O\}_n$ (1)

A mixture of $MnCl_2\cdot 4H_2O$ (12 mg, 0.05 mmol), $NaSO_3–H_2IPA$ (13.4 mg, 0.05 mmol), timb (15.9 mg, 0.05 mmol), DMA (1.5 mL), and $H_2O$ (1.5 mL) was stirred at room temperature for 15 min, then sealed in a 10 mL Teflon lined stainless steel vessel, and heated at 100°C for 2 days, followed by cooling to room temperature at a rate of 10°C·h$^{-1}$. Light yellow block-shaped crystals of **1** were obtained, washed with distilled water, and dried (yield 37.2%, based on $MnCl_2\cdot 4H_2O$). Anal. calcd for $C_{52}H_{62}Mn_3N_{12}O_{24}S_2$: C, 42.54; H, 4.26; $N$, 11.45; Found: C, 42.39; H, 4.15; $N$, 11.69%. FT-IR (KBr, $v$, cm$^{-1}$; s = strong, m = medium, w = weak, Figure S1): 3443w, 1650 s, 1573 s, 1402 s, 1226 m, 1131 m, 1000w, 733w, 665w.

The X-ray data were obtained by utilizing the Oxford Xcalibur E diffractometer. The intensity data was analyzed by utilizing the CrysAlisPro software and converted to the HKL files. The SHELXS program on the basis of direct approach was utilized to create the initial structural models, and the SHELXL-2014 program on the basis of the least-squares approach was modified.[15,16] The whole non-H atoms were mixed with anisotropic parameters. Then we utilized the AFIX commands to fix the whole H atoms geometrically on the C atoms that they attached. Table 1 details refinement details as well as crystallographic parameters of the complex **1**.

### Calcium colorimetric assay

Calcium Colorimetric Assay was conducted in this present research to measure the treatment activity of the compound on the renal calculus mice through measuring the concentration of the $Ca^{2+}$ in urine. This preformation was conducted totally under the guidance of the instructions with only a little change. In brief, 50 animals were used in this research, which were obtained from the Qingdao Municipal Hospital. Before the experiment, all the animals were cultured in the standard condition of 20–25°C, with free water and food. The animals were divided into five groups: the control group, model group, and compound treatment groups. The high-calcium diet containing oxalic acid was used to induce the renal calculus animal model, next the new compound was given for treatment at the concentrations of 1, 2, and 5 mg/kg. After that, the urine of all the mice was collected and the $Ca^{2+}$ concentration in urine was determined with Calcium Colorimetric Assay with three repeats.

### Western blotting assay

The western blotting assay was performed to evaluate the osteopontin expression levels in distal tubule. This conduction was carried out strictly in accordance with the manufacture instructions. In short, 50 animals were used in this research, which were obtained from the Qingdao Municipal Hospital. Before the experiment, all the animals were cultured in the standard

**Table 1.** Refinement details and crystallographic parameters for complex 1.

| Empirical formula | $C_{52}H_{46}Mn_3N_{12}O_{16}S_2$ |
|---|---|
| Formula weight | 1323.95 |
| Temperature/K | 293.15 |
| Crystal system | Monoclinic |
| Space group | I2/a |
| a/Å | 19.214(2) |
| b/Å | 11.462(5) |
| c/Å | 29.559(2) |
| $\alpha/°$ | 90 |
| $\beta/°$ | 107.026(4) |
| $\gamma/°$ | 90 |
| Volume/Å$^3$ | 6225(3) |
| Z | 4 |
| $\rho_{calc}$g/cm$^3$ | 1.413 |
| $\mu$/mm$^{-1}$ | 0.739 |
| 2$\Theta$ range for data collection/° | 5.44 to 50 |
| Index ranges | $-22 \leq h \leq 22, -13 \leq k \leq 13, -35 \leq l \leq 35$ |
| Reflections collected | 76,937 |
| Independent reflections | 5464 [$R_{int}$ = 0.0664, $R_{sigma}$ = 0.0310] |
| Data/restraints/parameters | 5464/0/388 |
| Goodness-of-fit on F$^2$ | 1.137 |
| Final R indexes [I > = 2$\sigma$ (I)] | $R_1$ = 0.0796, $\omega R_2$ = 0.1935 |
| Final R indexes [all data] | $R_1$ = 0.0938, $\omega R_2$ = 0.2012 |
| Largest diff. peak/hole/e Å$^{-3}$ | 0.85/−0.85 |
| CCDC | 2112125 |

condition of 20–25°C, with free water and food. The animals were divided into five groups: the control group, model group, and compound treatment groups. The high-calcium diet containing oxalic acid was used to induce the renal calculus animal model, next the new compound was given for treatment at the concentrations of 1, 2, and 5 mg/kg. After that, the distal tubule tissue was harvested and the Total Protein Extraction kit was used to extract the total protein in the cells. The BCA Protein Assay Kit was used to measure the total protein concentration. All the samples were separated by SDS-PAGE gel electrophoresis and electrophoretically transferred to a 0.22 mm polyvinylidene fluoride (PVDF) membrane. After incubated with primary antibody (OPN or GAPDH) and appropriate secondary antibody conjugated with horseradish peroxidase, the protein images were captured.

## Simulation methods

The molecular docking simulation has been prepared by AutoDockTools 1.5.6 and performed by AutoDock 4.2. The biological antibody 23C3 has been employed as the receptor protein for investigating the possible binding interactions with the Mn complex, the structure of the antibody was downloaded from protein data bank, and the corresponding PDB ID is 3CXD.[17] The grid box that includes the docking pocket locates at the center of mass of the 3CXD structure, and detailed coordination of the center of mass is −8.314, 15.77, −29.053 (Å). The number of grid points in each

direction is 60, and the spacing length is 0.375 Å. Only the polar hydrogens on the 3CXD protein are considered explicitly, during the docking simulation, the structure of the receptor is rigid, but the structure of the Mn complex is semi-flexible; thus, 9 torsional degrees of freedom are allowed for adjusting the conformation of Mn complex inside the docking pocket. The maximum allowed molecular docking run is set to 60 and the scoring method is Lamarckian Genetic algorithm (LGA).

## Results and discussion

### *Structural characterization*

Single crystal X-ray diffraction analysis reveals that **1** crystallizes in the monoclinic crystal system of *C*2/*c* (15). The asymmetric unit of **1** contains two crystallographically distinct divalent Mn atoms, one timb linker, one $SO_3$–$IPA^{2-}$ ligand, and one coordinated and four lattice water molecules. The occupancies are 1 for Mn1 and 0.5 for Mn2. Mn1 is located in a distorted $\{MnN_3O\}$ tetrahedral geometry ($\tau_4 = 0.85$), completed by three imidazolyl N atoms (*N*1, *N*3A, and *N*6B) from three different timb linkers and one carboxyl O atom (O2) from an $SO_3$–$IPA^{2-}$ ligand. Mn2 is centrosymmetric and hexacoordinated by four carboxyl O atoms (O3, O4, O3C, and O4C) from two $SO_3$–$IPA^{2-}$ ligands and two oxygen atoms from two coordinated water molecules (O8 and O8C), leaving a distorted $\{MnO_6\}$ octahedral geometry (Figure 1(a)). Besides, the Mn–O bond lengths are in the range of 1.924(5)–2.194(7) Å, and the Mn–N bond lengths span from 1.999(5) to 2.014(5) Å, respectively. The bond angles around MN(II) in **1** are from 61.3(2) to 118.7(2)°. Interestingly, the timb ligands act as tripodal linkers to connect Mn1 ions to give a 2D $[Mn_3(timb)_2]_n$ sheet in **1** (Figure 1(b)), with the Mn1⋯Mn1 distances being 10.432, 11.530, and 12.462 Å, respectively. The $SO_3$–$IPA^{2-}$ ligands act as pillars by adopting the $(\kappa^1$-$\kappa^0)$-$(\kappa^1$-$\kappa^1)$-$\mu_2$ coordination mode and sustain the 2D $[Mn_3(timb)_2]_n$ sheets to form a bilayer structure (Figure 1(c)). The bilayers further interpenetrate with each other to finally give a 2D + 2D → 3D interpenetrating net (Figure 1(d)). Besides, the lattice water molecules occupy the channels of the 2D + 2D → 3D interpenetrating net through the O–H⋯O hydrogen bonds. The total potential solvent area volume of **1** is 1035.2 Å$^3$ for per cell unit of 6377.0 Å$^3$ (16.2% of the total crystal volume) after the removal of free solvent molecules calculated using PLATON. Topologically speaking, the bilayer structure of **1** can be considered as a 2-nodal (3,4)-connected sheet with the stoichiometry (3-c) (4-c) by donating the Mn1 ions to be 4-connected nodes and the timb linkers to be 3-connected nodes, respectively.

### *Reduced concentration of the $Ca^{2+}$ in urine in a dose- and time-dependent manner after compound exposure*

In the procession of renal calculus, the $Ca^{2+}$ in the urine plays an important role. Thus, the Calcium Colorimetric Assay was firstly conducted in this present research to measure the concentration of the $Ca^{2+}$ in urine after compound treatment. As the results showed in Figure 2, we can see that, in the model group, there was a much higher level of the $Ca^{2+}$ concentration, which is significantly different from the control group. After the treatment of the new compound, the increased level of $Ca^{2+}$ in urine was significantly reduced in a dose- and time-dependent manner, suggesting the excellent biological activity of the new compound on renal calculus therapy.
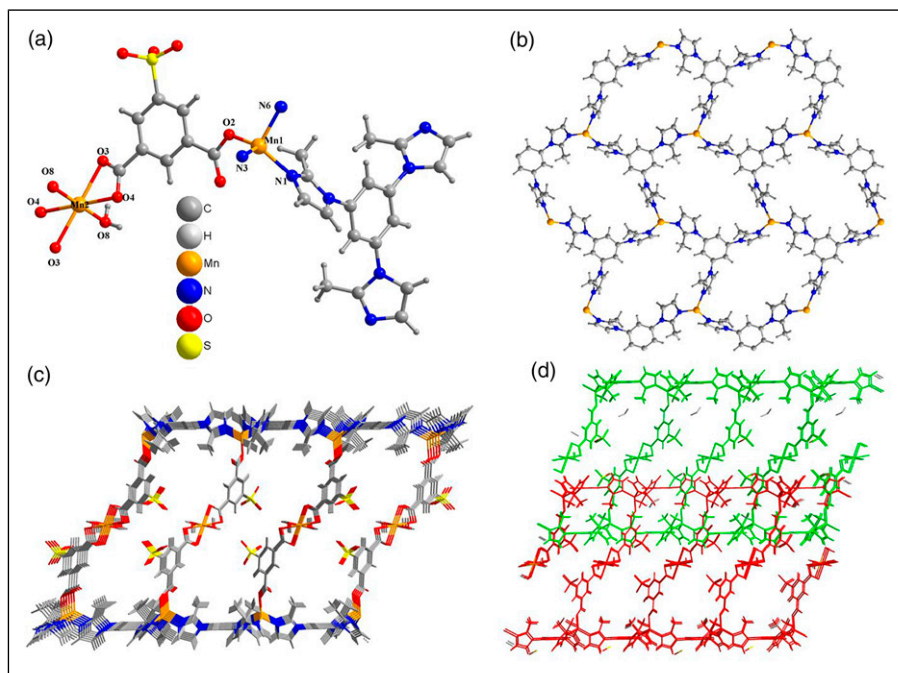
**Figure 1.** (a) A view of the contents of the asymmetric unit. (b) 2D $[Mn_3(timb)_2]_n$ sheet in **1**. (c) The bilayered structure of **1**. (d) The 2D + 2D → 3D interpenetrating net of **1**.
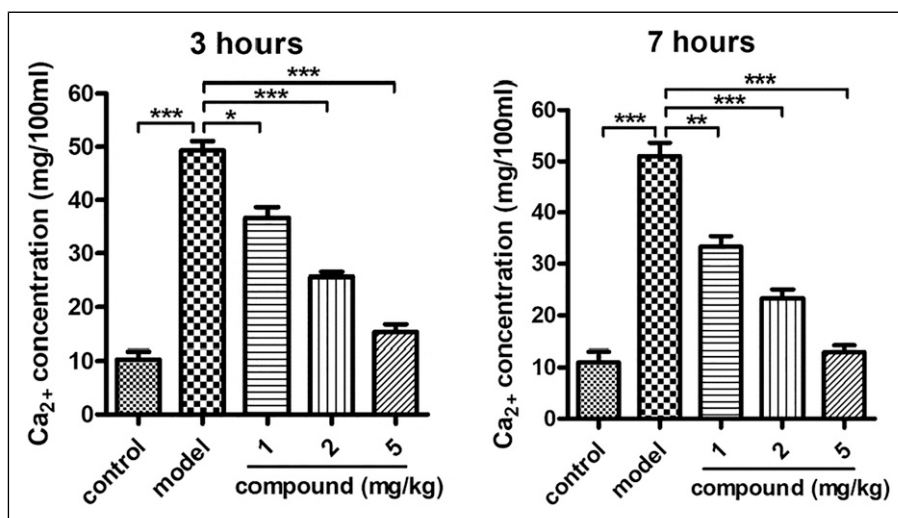


**Figure 2.** Compound reduced the concentration of the $Ca^{2+}$ in urine in a dose- and time-dependent manner. The high-calcium diet containing oxalic acid was used to induce the renal calculus animal model, next the new compound was given for treatment at the concentrations of 1, 2, and 5 mg/kg. Calcium Colorimetric Assay was used to measure the $Ca^{2+}$ concentration in the urine.

## Inhibited expression levels of the osteopontin in distal tubule after compound treatment

As previously reported, the osteopontin plays an important role in cell matrix remodeling, tissue calcification, pro-inflammatory cytokines, and cell apoptosis regulation. In recent years, it has been confirmed that osteopontin is closely related to the formation of urinary stones. In the above research, we also proved that the new compound has excellent inhibitory effect on the $Ca^{2+}$ concentration in the urine. Thus, in this research, western blotting assay was further conducted and the expression levels of the osteopontin in distal tubule were evaluated. In Figure 3, we showed that, the level of the osteopontin expression in the model group was much higher than that of the control group. After the treatment of the new compound, osteopontin expression was reduced in a dose-dependent manner.

## Molecular docking

It is well-known that osteopontin plays a key role in the development and perpetuation of related disease, and antibodies that are targeting the osteopontin have shown effective therapeutic benefits for the curing of related disease.[17] Thus, the biological antibody 23C3 has been chosen to be the receptor protein for probing the biological activity of the newly synthesized Mn complex. 60 binding poses have been generated randomly and scored by the LGA methods during the molecular docking simulation; the binding conformation that exhibits the lowest affinity energy ($-14.6$ kcal/mol) among the 60 binding poses is displayed in Figure 4.

It can be seen from Figure 4 that five binding interactions have been formed between the Mn complex and the receptor protein. All types of polar groups on the Mn complex are able to form hydrogen bonding interactions with the active sites (polar hydrogens) inside the docking pocket. Explicitly, the carboxyl group interacts with residue LYS-142 with a hydrogen bond length of 1.7, the iminazole group interacts with residue VAL-155 and the hydrogen bond length is 2.0, the sulfonate group interacts with residues LYS-103 and GLN-166, interestingly, all three oxygen atoms on the sulfonate group are interacting with the active site, and the
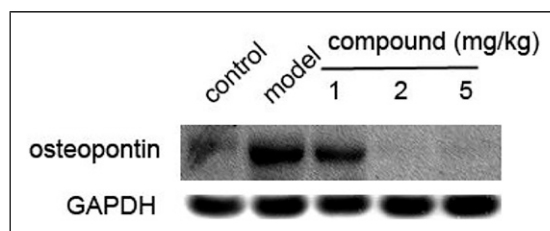


**Figure 3.** Compound inhibited the expression of the osteopontin in distal tubule. The high-calcium diet containing oxalic acid was used to induce the renal calculus animal model, next the new compound was given for treatment at the concentrations of 1, 2, and 5 mg/kg. Western blotting assay was conducted and the osteopontin expression evaluation in distal tubule was measured after compound exposure.
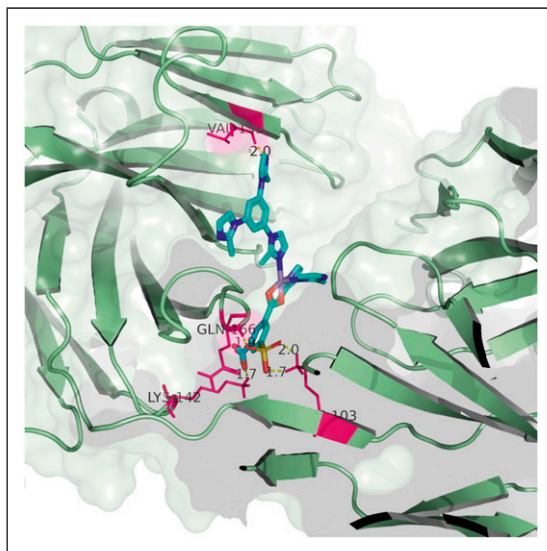
**Figure 4.** The binding conformation that exhibits the lowest affinity energy ($-14.6$ kcal/mol) among the 60 binding poses, and the estimated inhibition constant is 1.37 nM. Four active residues (pink) are involved in the binding interactions with the Mn complex, and five hydrogen bonds are formed.

formed hydrogen bond lengths are 1.7 and 2.0 to residue LYS-103 and 1.9 to residue GLN-166. The above results suggest that the Mn complex has excellent biological activity and agree well with the experimental results.

## Conclusion

In summary, we have prepared a two-dimensional Mn(II) coordination polymer via using the mixed-ligand synthesis approach by reaction of $MnCl_2\cdot4H_2O$ with the tripodal linker 1,3,5-tris(2-methylimidazol-1-yl)benzene and aromatic dicarboxylic acid ligand $-SO_3$ group functionalized isophthalic acid ligand. The as-prepared coordination polymer **1** has been structurally studied via the single crystal X-ray diffraction and was further characterized by elemental analysis. The data of the Calcium Colorimetric Assay exhibited that the compound could significantly reduce the concentration of the $Ca^{2+}$ in urine in a dose- and time-dependent manner. In addition to this, the results of western blotting assay suggested that the compound inhibited expression levels of the osteopontin dose dependently. Above all, we draw this conclusion that the compound could be an excellent candidate for the renal calculus therapy by reducing the levels of $Ca^{2+}$ in urine and osteopontin expression in distal tubule. Molecular docking simulation found that the carboxyl group, the iminazole, and sulfonate groups are all able to form binding interactions with the active sites inside the docking pocket, and the formed hydrogen bond lengths are relatively short and therefore indicate strong biological activity.

### Declaration of conflicting interests

The author(s) declared no potential conflicts of interest with respect to the research, authorship, and/or publication of this article.

## Funding

## Supplemental material

Supplemental material for this article is available online.

## References

1. Fan L, Zhao D, Li B, et al. Luminescent binuclear Zinc(II) organic framework as bifunctional water-stable chemosensor for efficient detection of antibiotics and Cr(VI) anions in water. *Spectrochim Acta A Mol Biomol Spectrosc* 2022; 264: 120232.

2. Fan L, Zhao D, Li B, et al. An exceptionally stable luminescent cadmium(ii) metal–organic framework as a dual-functional chemosensor for detecting Cr(vi) anions and nitro-containing antibiotics in aqueous media. *CrystEngComm* 2021; 23: 1218–1225.

3. Wang F, Tian F, Deng, et al. Cluster-based multifunctional copper(II) organic framework as a photo-catalyst in the degradation of organic dye and as an electrocatalyst for overall water splitting. *Cryst Growth Des* 2021; 21: 4242–4248.

4. Li RF, Liu XF, Zhang T, et al. Hydrothermal syntheses, structures, and magnetic properties of two new Mn(II) complexes with biphenyl-2,3,3′,5′-tetracarboxylic acid. *J Mol Struct* 2014; 1075: 456–461.

5. Li RF, Gu YX, Liu XF, et al. Syntheses, structures, and properties of two zinc(ii) metal-organic frameworks based on biphenyl-2,3,3′,5′-tetracarboxylic acid and N-donor ancillary ligands. *Z Anorg Allg Chem* 2015; 641: 1114–1118.

6. Hu ML, Razavi SA, Piroozzadeh M, et al. Sensing organic analytes by metal-organic frameworks: a new way of considering the topic. *Inorg Chem Front* 2020; 7: 1598–1632.

7. Hu ML, Safarifard V, Doustkhah E, et al. Taking organic reactions over metal-organic frameworks as heterogeneous catalysis. *Micropor Mespor Mat* 2018; 256: 111–127.

8. Wang MF, Mi Y, Hu FL, et al. Coordination-driven stereospecific control strategy for pure cycloisomers in solid-state diene photocycloaddition. *J Am Chem Soc* 2020; 142: 700–704.

9. Bharati AK, SomnathLama P, Lama P, et al. A novel mixed ligand Zn-coordination polymer: Synthesis, crystal structure, thermogravimetric analysis and photoluminescent properties. *Inorg Chim Acta* 2020; 500: 119219.

10. Shi YS, Hao ZC, Han C, et al. Synthesis, crystal structures, and luminescence sensing properties of two metal complexes containing bis(thiabendazole) moieties. *J Mol Struct* 2020; 1201: 127218.

11. Gao L, Zhang J, Zhai L, et al. Fluorescent sensing properties of Cd(II)/Zn(II) metal-organic frameworks based on 3,5-di(2′,5′-dicarboxylphenyl)benozoic acid. *Polyhedron* 2019; 164: 90–95.

12. Wang J, Chen NN, Zhang C, et al. Functional group induced structural diversities and photocatalytic, magnetic and luminescence sensing properties of four cobalt(ii) coordination polymers based on 1,3,5-tris(2-methylimidazol-1-yl)benzene. *CrystEngComm* 2020; 22: 811–820.

13. Fouad R. Synthesis and Fundamental Characterization of Diverse Properties of Biocompatible Cd (II) Phosphor Complex for Cytotoxic Activity and Latent Fingerprint Detection. *Appl Organomet Chem* 2020; 34: 23–26.

14. Sen R, Halder A and Ghoshal D. Three mixed ligand coordination polymers: Syntheses, characterization and detailed study of the structural transformations. *Polyhedron* 2020; 183: 114534.

15. Sheldrick GM. SHELXT- Integrated space-group and crystal-structure determination. *Acta Crystallogr Sect A Found Adv* 2015; 71: 3–8.

16.  Sheldrick GM. Crystal structure refinement withSHELXL. *Acta Crystallogr Sect C Struct Chem* 2015; 71: 3–8.

17.  Du J, Hou S, Zhong C, et al. Molecular basis of recognition of human osteopontin by 23C3, a potential therapeutic antibody for treatment of rheumatoid arthritis. *J Mol Biol* 2008; 382: 835–842.